Comparative study of the contact pressures in hip joint models with femoroacetabular impingment with different cephalic deformities

Iryna Havenko

Instituto Superior Técnico, Universidade de Lisboa, Portugal

October 2017

Abstract

In this study, finite element analyses of hip joint models with femoroacetabular impingment of the cam-type are performed. For comparative purposes, patient-specific three-dimensional geometries of the hip joint structures are obtained by manual segmentation from arthro-MRI sequences of images in two pathologic cases presenting different cephalic deformities characterized by alpha-angles equal to 60º and 81º, respectively. In the numerical simulations, the pathologic hip joints are submitted to a physiological compression force and to several physiological hip motions. In all the analyses the bony structures are considered rigid and the soft tissues are considered as linear elastic and isotropic materials. The contact pressures and the von Mises stresses are registered and compared in these pathologic hip models in order to better understand the mechanism of aggression of the intra-articular tissues and to justify and validate the current medical treatment. Moreover, this study aims at understanding the role of the labrum in the pathologic hip joints. Thus, numerical simulations of the hip models without the presence of the labral tissue are also performed.The magnitudes of the contact pressures obtained in the two pathological cases are in coherence with published data and are higher than the ones obtained in normal hip joints. As a consequence of the increased severity of the cam impingement, increased contact pressure magnitudes are observed in the pathologic hip with larger alpha angle. When the labrum is absent from the model, the magnitudes of the contact pressures are moderately smaller than the ones obtained in the complete models. However, the regions that are now subjected to pressure are wider, suggesting that the labrum has a supportive and protective action that preserves some regions of the cartilage structures from high pressures.

Keywords: femoroacetabular impingement, cam impingement, osteoarthritis, hip joint, alpha angle, femoral cartilage, acetabular cartilage, labrum, finite element analysis, 3D reconstruction

1. Introduction

The hip joint is one of the most important human joints in the body. The complexity of its anatomical and functional specifications provides equilibrium and balance, resulting in notorious firmness and permitting different motions with a broad range in distinct anatomical planes. It plays a major role in the gait cycle, and in the normal daily living activities. The structure of this type of joint promotes the accommodation of the human body weight and allows the spreading of the loads on the body.

The femoroacetabular impingement (FAI) in the hip joint is an abutment mechanism, due to the abnormal hip morphology, between the femoral head/neck and the acetabular rim, resulting in cartilage and labrum aggression. Mostly prevalent in active adults, the individuals usually reveal hip pain and decreased hip mobility [1][2]. As a result of the abnormal (non-physiological) stresses and contact pressures experienced within the intra-articular structures, this pathological mechanism may lead to hip dysfunction. The pathological mechanism of FAI has been commonly associated as a potential cause of cartilage degeneration and posterior development of early osteoarthritis (OA) of the hip. Early diagnosis and accurate treatment should be performed in order to avoid extreme cartilage damage and to improve the patient's mobility and life quality [3].

There are two types of impingement distinguished so far: the cam-type impingement and the pincer-type impingement. The former is characterized by an abnormal (non-spherical) shape of the femoral head with decreased femoral head/neck offset. The latter, is characterized by an abnormal local or global overcoverage of the acetabulum [4]. Mixed impingement can also be observed. Cam-type lesions mostly affect the articular cartilage and may lead to labrum tear. Pincer-type lesions affect predominantly the labral tissue.

FAI of the cam-type impingement, the focus in this study, is characterized by an abnormal value of the alpha angle, a geometrical parameter. The alpha angle is a measurable anatomical characteristic of the hip morphology and quantifies the morphological deformity of the femoral head. Normal hip morphology is characterized by alpha angles in the range of 40-50º [5]. The deformity in the femoral head is located usually at the anterosuperior rim and the repetitive impacts between the abnormal femoral head and the acetabulum lead to excessive stresses and contact pressures in the intra-articular structures [6]. Mostly prevalent in young athletic male adults, the femoroacetabular (FAI) of the cam-type is observed when the hip is submitted to flexion and internal rotations movements, required in intense sports activities and also in normal routine activities. For advanced cam-type impingement, individuals usually present pain and limited hip motions when submitted to experimental clinical tests. Currently, imaging techniques such as magnetic resonance imaging arthrograms (arthro-MRI) are performed to identify the cam-type abnormality in the hip and to assess the severity of the aggression of the soft tissues. More extensive diagnosis may

be useful to identify, in some cases, cartilage inflammation and chondromalacia [6]. The treatment of FAI of the cam-type is mainly surgical. It consists on restoring the sphericity of the femoral head, by trimming the aspherical shape observed on the femoral head/neck junction and can be done by open surgery or by arthroscopy [7].

The goal of this study is to compare the intra-articular von Mises stresses and contact pressures in hips with femoroacetabular impingement of the cam-type with various degrees of morphological deformity, with and without the presence of the labral tissue aiming at improving and validating the current treatment techniques. Individuals with FAI of the cam-type with distinct values of alpha angles are considered in order to assess its influence on the values of the stresses and contact pressures and the consequent intensity of the aggression of the soft tissues (articular cartilages and labrum). The patient-specific real geometries of the hip joint are obtained from arthro-MRI sequences of images. Based on the same reconstruction method as used in Lourenço et al. [9], three-dimensional (3D) finite element (FE) meshes of the femoral cartilage, acetabular cartilage and labrum are obtained, and the corresponding models are analysed under the action of physiological hip forces and physiological rotational motions.

The finite element (FE) contact analyses in real patient-specific geometry models, comparatively to those performed in idealized/artificial models [5], provides a personalized diagnosis and treatment procedure for each individual. Thus, this study, in our opinion, will help to justify and validate the current medical treatment interventions that delay the aggression of the soft tissues and its progression eventually resulting in OA. Also, this study aims at understanding the role of the labrum in the pathologic hip joints.

2. Reconstruction Methodology

In the present work, models of the hip of two patients presenting cam impingement with distinct alpha angles of 60º and 81º were analyzed. For the purpose, two sets of arhtro-MRI sequence images with 16 radial images of the pathologic hip joints, with gadolinium injection, were provided by an orthopaedical surgeon. The 3D reconstruction of the hip joints models and the FE analysis were performed using the following methodology already validated in [8] [9]: manual image segmentation, surfaces and posterior solid creation, and finite element mesh generation and analysis. The first case analyzed corresponds to a male patient presenting a cam-type femoroacetabular impingement with an alpha angle of 60º. The image acquisition was performed radially, with radial angle increment of 11.25º, varying from 0º to 180º and the rotational axis was coincident with the axis that defines the femoral neck and extends to the femoral head.

The manual segmentation steps and the 3D reconstruction of the hip joint models were performed using the same, already validated procedures, as in [8][9]. For the segmentation purposes,

Rhinocerus software was used in order to obtain the contours of the anatomical structures of interest and the posterior extraction of geometrical data relative to the structures that define the pathologic hip joint. The main components are: the femur (green), the acetabulum and pelvic bone (red), the femoral cartilage (blue, green and red), the acetabular cartilage (red, cyan, blue and magenta) and the labrum (magenta, red and blue). In order to obtain the 3D reconstruction of the structures of interest, subcurves from the existing curves delimiting the anatomical components were created. The reconstructed soft tissues and the respective isocurves are represented in Figure 1 and the final 3D model of the hip joint in Figure 2.

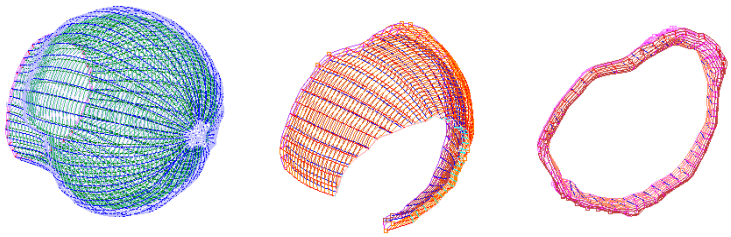

Figure 1: Case 1 - 3D representation of the anatomical structures formed by the circumferential isocurves. From left to right: femoral cartilage, acetabular cartilage and labrum.

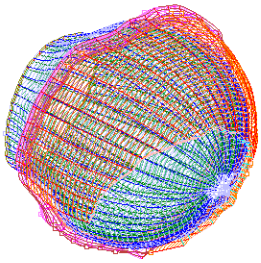

Figure 2: Case 1 - Final 3D model, obtained in Rhinocerus, representing the fully constructed model of the soft tissues of the hip joint.

Regarding the surfaces creation and the development of the solid model for each of the components of the soft structures, geometrical information was extracted from the final assembly represented in Figure 2. The cloud point interpolation was performed using FastRBF (Fast Radial Basis Functions) toolbox especially designed for MATLAB, enabling the reconstruction and representation of the surfaces of interest. The surfaces obtained from fastRBF toolbox were generated as .obj files. In order to create the three-dimensional solid models of each anatomical component, the .obj files were assessed using the Solidworks software. The complete FE mesh of the model of the hip joint that was used in the numerical simulations was obtained using Abaqus software and is represented in Figure 3 (left) and has a total of 288641 tetrahedral mesh elements. Different mesh colors were assigned to each anatomical component of the hip joint in order to be straightforwardly distinguishable. The same reconstruction

methodology was used for the pathologic case 2. The total number of tetrahedral mesh elements used for numerical simulation purposes in this case was 363739 and the final mesh is presented in Figure 3 (right).

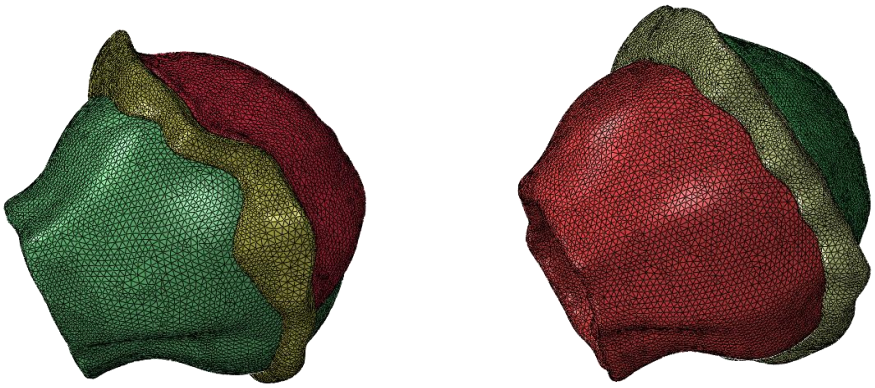

Figure 3: Left: Case 1 - Complete FE mesh of the three structures of the hip joint (total number of elements: 288641). Green – femoral cartilage; Red – acetabular cartilage; Yellow – labrum. Right: Case 2 - Complete FE mesh of the three structures of the hip joint (total number of elements: 363739. Red – femoral cartilage; Green – acetabular cartilage; Yellow – labrum.

3. Finite element analysis

The numerical analyses were performed using Abaqus software and all the analyses were geometrically non-linear. Regarding structural constraints of the two models (case 1 – alpha angle equal to 60º and case 2 – alpha angle equal to 81º with and without labrum), the displacements of the outer nodes of the surface of the acetabular cartilage and of the outer part of the acetabular labrum, that are in contact with the acetabulum bone, were restricted. The regions of the acetabular cartilage and the labrum that are in contact were tied forming a singular contact surface. The contact between the merged surface of the acetabular cartilage and labrum with the surface of the femoral cartilage was considered frictionless. The nodes of the inner surface of the femoral cartilage were rigidly constrained to the node in the centroid of the femoral head. Moreover, an anatomical orientation was assigned to each hip joint model in order to simulate a physiological normal orientation of the femur in the human body (the anatomical orientation for each model of the hip joint was previously obtained from a detailed MATLAB script using geometrical data from the manual segmentation from Rhinocerus).

For the simulation purposes, all the analyses were performed considering that all the patients have a BW of 750N and thus, the compression force simulating the normal daily walking activity has a y-component of 1875N and x-component of 450N. Regarding the rotational motions applied to the pathologic hip joints, and being the hip joints subjected to the compression force mentioned above, i) the pure internal rotation was performed with an angle of 45º (along y-axis) and ii) the flexural rotation (along x-axis) was performed with an angle of 90º. Regarding the rotational motions, and in order to evaluate the

contact pressures in different regions of the femoral cartilage, some nodes were selected along the femoral cartilage. For the pure internal rotation, some nodes were selected defining a straight line, perpendicular to the rotation axis (y-axis), and for the flexural rotation, some nodes were selected also defining a straight line perpendicular to the rotation axis (x-axis). The nodes were selected in the region of the cam protuberance for the two pathologic hip joints.

In Table 1 and Table 2, the maximum magnitudes of the contact pressures on the femoral cartilage (FC), acetabular cartilage (AC) and labrum (L) after the pure flexural rotation of 90º and pure internal rotation of 45º, are presented, respectively.

Table 1: Case 1 – Magnitudes of the contact pressures registered on the three hip components during and at the end of the flexural rotation step.

		Contact Pressure	
		Maximum during step	**Final Maximum**
Flexural rotation 90º	**FC**	**8.653 MPa** (70% of the step) I region	**7.425 MPa** S region
	AC	**13.79 MPa** (35% of the step) P region	**5.666 MPa** S region
	L	**12.42 MPa** (100%) I region	**12.42 MPa** S region

Table 2: Case 1 – Magnitudes of the contact pressures registered on the three hip components during and after the internal rotation step.

		Contact Pressure	
		Maximum during step	**Final Maximum**
Internal rotation 45º	**FC**	**14.77 MPa** (70% of the step) I region	**10.45 MPa** I region
	AC	**13.61 MPa** (100%) P region	**13.61 MPa** P region
	L	**18.44 MPa** (55% of the step) PI region	**10.96 MPa** P region

The contact pressures on the nodes selected perpendicularly to the flexural rotation axis are presented in Figure 4 as a function of the angle of rotation. The final maximum contact pressure observed on the femoral cartilage (7.425 MPa) does not occur in any of the selected nodes. It occurs near the node F3, which presents a maximum value of 4.954 MPa.

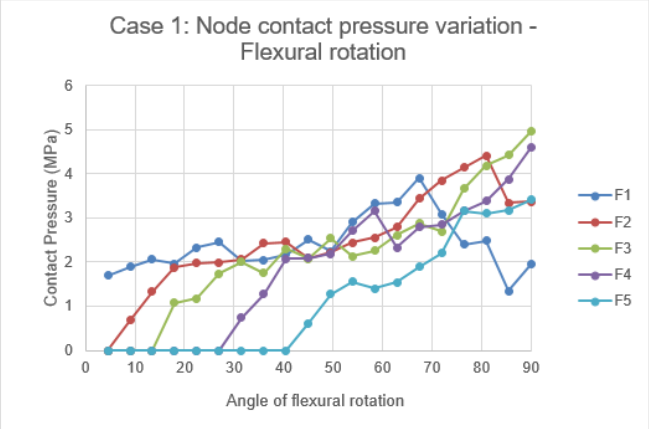

Figure 4: Case 1 - Contact pressures evolution in the selected nodes of the femoral cartilage as a function of the angle of flexural rotation.

Evolution of the contact pressures on the selected nodes is presented as a function of the angle of internal rotation (see Figure 5). The final maximum contact pressure observed on the femoral cartilage (10.45 MPa) does not occur in any of the selected nodes. The measured local value of 8.44 MPa on the AS region is coeherent with the contact pressures in node R2, which presents a maximum magnitude of 8.908 MPa.

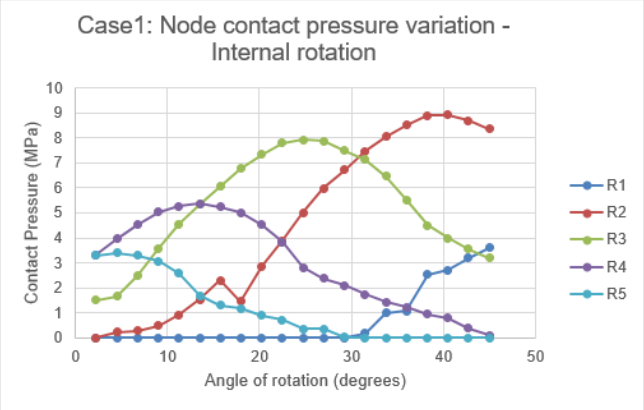

Figure 5: Case 1 - Contact pressure evolution in the selected nodes on the femoral cartilage as a function of the angle of pure internal rotation.

For case 2, in Table 3 and Table 4, the final maximum magnitudes of the contact pressures on the femoral cartilage (FC), acetabular cartilage (AC) and labrum (L) after the pure flexural and pure internal rotation are presented.

Table 3: Case 2 – Magnitudes of the contact pressures registered on the three hip components during and at the end of the flexural rotation step.

		Contact Pressure	Von Mises
		Final Maximum	Final Maximum
Flexural rotation 23.4º	FC	53.68 MPa I region	7.043 MPa I region
	AC	10.88 MPa I region	10.11 MPa I region
	L	57.45 MPa I region	11.89 MPa I region

Table 4: Case 2 – Magnitudes of the contact pressures registered on the three hip components during and after the internal rotation step.

		Contact Pressure	
		Maximum during step	Final Maximum
Internal rotation 45º	FC	36.84 MPa (35% of the step) I region	9.775 MPa AS region
	AC	10.12 MPa (50% of the step) AS region	9.158 MPa AS region
	L	51.40 MPa (45% of the step) AI region	17.59 MPa AS region

The plot that describes, for case 2, the evolution of the contact pressures in the selected nodes as a function of the angle of internal rotation can be observed in Figure 6. The final maximum contact pressure observed on the femoral cartilage (9.775 MPa) does not occur in any of the selected nodes. It occurs near node R3 which presents a maximum value of 7.65 MPa.

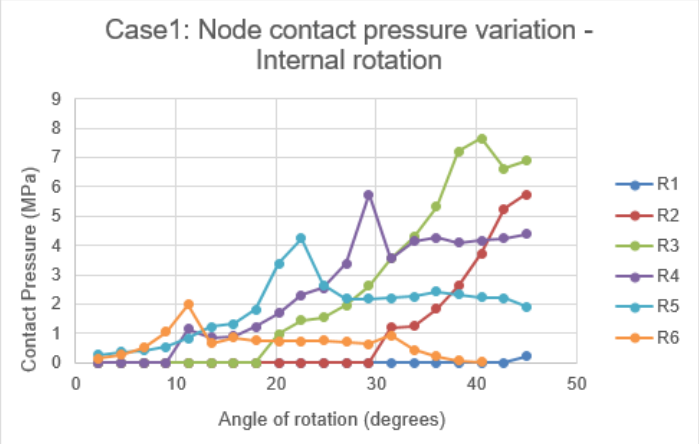

Figure 6: Case 2 - Contact pressures evolution in the selected nodes on the femoral cartilage as function of the angle of pure internal rotation.

4. Conclusions

This section aims to analyze and compare the values obtained from the numerical simulations of the two pathological cases with distinct degrees of the cam deformity (with alpha angles of 60º and 81º, respectively) and also to evaluate the effect of the absence of the labral tissue in the hip joints. Validation of the results with already existing data [8] [9] is also performed.

The main objectives of the performed analysis are a) to compare the intra-articular von Mises stresses and contact pressures in hips with femoroacetabular impingement of the cam-type with various degrees of morphological deformity, b) to evaluate the effect of the abscence of the labral tissue in hip joints in order to c) validate the current treatment techniques.

The magnitudes of the contact pressures obtained in the two pathological cases are in coherence with published data and are higher than the ones obtained in normal hip joints. As a consequence of the increased severity of the cam impingement, increased contact pressure magnitudes are observed in the pathologic hip with larger alpha angle. For the imposed physiological rotational motions, the internal rotation appears to be the determinant hip joint motion for the genesis of the high intra-articular contact pressures. For the pure flexural rotation, it was not possible to compare the effect of the alpha-angle since the FE analysis for case 2 did not converge. However, higher magnitudes of the contact pressure were obtained in case 2, with higher alpha angle, when compared with the magnitudes obtained in case 1 for the same flexural loading. For the pure internal rotation, in both cases, the obtained contact pressures on the femoral and acetabular cartilages are higher when comparing with normal hips. In case 2, with higher alpha angle, the obtained contact pressures in the femoral cartilage and in the labrum are higher when comparing with case 1. It is thus conclusive that the tissue aggression is influenced by the severity of the cam-type impingement in pathologic hip joints; major intra-articular pressures and stresses are observed in the hip of the patient with alpha angle equal to 81º than in the hip of the patient presenting an alpha angle equal to 60º. When the labrum is absent from the model, the magnitudes of the contact pressures are moderately smaller than the ones obtained in the complete models. However, the regions that are now subjected to pressure are wider, suggesting that the labrum has a supportive and protective action that preserves some regions of the cartilage structures from high pressures. In the cases where the labral tissue is damaged, an early surgical intervention may also be a key aspect in preventing major joint degeneration.

This study confirms the abnormal functioning of the hip joints with cam-type impingement. The increased magnitudes of the contact pressures on the intra-articular structures may justify the origin of the observed damage, and thus, the early surgical intervention may prevent the outset of the articular

complications. Regarding the future developments, major achievements in the simulations may be accomplished by considering the bony structures as non-rigid materials (elastic materials) and the cartilages as porous materials. Also, including the tissues that surround the hip joint such as ligaments, would represent a hip joint environment more consistent with reality.

References

[1] M. Leunig, P. E. Beaulé, and R. Ganz, “The concept of Femoroacetabular impingement: Current status and future perspectives,” *Clin. Orthop. Relat. Res.*, vol. 467, no. 3, pp. 616–622, 2009.

[2] S. Wagner *et al.*, “Early osteoarthritic changes of human femoral head cartilage subsequent to femoro-acetabular impingement,” *Osteoarthr. Cartil.*, vol. 11, no. 7, pp. 508–518, 2003.

[3] R. Ganz, M. Leunig, K. Leunig-Ganz, and W. H. Harris, “The etiology of osteoarthritis of the hip: An integrated mechanical concept,” *Clin. Orthop. Relat. Res.*, vol. 466, no. 2, pp. 264–272, 2008.

[4] J. Parvizi, M. Leunig, and R. Ganz, “Femoroacetabular Impingement,” *J. Am. Acad. Orthop. Surg.*, vol. 15, no. 9, pp. 561–570, 2007.

[5] S. Chegini, M. Beck, and S. J. Ferguson, “The effects of impingement and dysplasia on stress distributions in the hip joint during sitting and walking: A finite element analysis,” *J. Orthop. Res.*, vol. 27, no. 2, pp. 195–201, 2009.

[6] B. D. Kuhns, A. E. Weber, D. M. Levy, and T. H. Wuerz, “The Natural History of Femoroacetabular Impingement,” *Front. Surg.*, vol. 2, no. November, pp. 1–7, 2015.

[7] P. Banerjee and C. R. McLean, “Femoroacetabular impingement: A review of diagnosis and management,” *Curr. Rev. Musculoskelet. Med.*, vol. 4, no. 1, pp. 23–32, 2011.

[8] J. P. Jorge *et al.*, “Finite element simulations of a hip joint with femoroacetabular impingement.,” *Comput. Methods Biomech. Biomed. Engin.*, vol. 17, no. 11, pp. 1275–1284, 2014.

[9] J. Lourenço, F. M. F. Simões, and P. A. Rego, “Finite element analyses of femoroacetabular impingement before and after hip arthroscopy.,” *Biomed. Mater. Eng.*, vol. 26, no. 3–4, pp. 193–206, 2015.